

Quantum mechanics calculation and Vibrational Spectra FT-IR and FT-Raman (theoretical, Experimental) studies of 5- Methyl-1H-Tetrazole (5MTZ)

A.Rajeswari^a, M.K. Murali^{a,*}, A.Ramu^b.

^a PG and Research department of physics, JJ.College of Arts & Science
(Autonomous), Pudukottai-622422, Tamil Nadu, India.(Affiliated Bharathidasan
university.Thiruchirappalli-620024.)

^b Department of Physics, Ganesar College of Arts and Science, Melaisivapuri-622403,
Tamil Nadu, India.

Article Info

Volume 83

Page Number: 139-156

Publication Issue:

September/October 2020

Abstract

The spectra of 5-Methyl-1H-tetrazole(5MTZ) have been recorded in the regions 4000–400 cm^{-1} for FT-IR and 3500–100 cm^{-1} for FT-Raman. The geometry optimization, vibrational frequencies were obtained by the density functional theory (DFT) using B3LYP method with 6-31G and 6-311+G basis sets. The complete assignments were performed on the basis of the potential energy distribution (PED) of the vibrational modes, calculated and the scaled values were compared with experimental FT-IR and FT-Raman spectra. The HOMO and LUMO energy gap reveals that the energy gap reflects the chemical activity of the molecule. The dipole moment (μ), polarizability (α), anisotropy polarizability ($\Delta\alpha$) and first hyperpolarizability (β_{tot}) of the molecule have been reported. Information about the size, shape, charge density distribution and site of chemical reactivity of the molecule has been obtained by molecular electrostatic potential (MEP).

Keywords: 5-Methyl-1H-tetrazole, DFT, FT-IR, FT-Raman, MEP

Article History

Article Received: 4 June 2020

Revised: 18 July 2020

Accepted: 20 August 2020

Publication: 15 September 2020

Introduction

The Quantum mechanics is used as a tool to learn the molecular forces determining

drug activity. This information can be used to infer the nature of the biological substances with which the drug reacts and

hopefully as a guide to the synthesis of useful new agents[1].the complete investigation of the 5-Methyl-1H-tetrazole(5MTZ) has been carried by DFT method,which belongs to the quantum mechanics.

In recent years, tetrazole and their derivatives have been extensively studied as they exhibit effective biological activities such as anti-inflammatory[2], antiviral[3], analgesic[4], antibacterial[5], antitubercular[6], anticonvulsant[7] etc. the title molecule 5-Methyl-1H-tetrazole is one of the tetrazole derivatives which used in the preparation of novel antifungal agents based derived from N-iodopropargylazoles and N-triiodoallylazoles. 5-Methyl Tetrazole also in the preparation of novel quinoline derivatives against mycobacterium tuberculosis. In these studies, the molecular structure, vibrational spectra and HOMO-LUMO energy gap of 5-Methyl-1H-tetrazole(5MTZ) were investigated by a concerted approach using matrix isolation vibrational spectroscopy and high-level DFT-based theoretical calculations. Regarding their studies, tetrazoles have been found to be extremely interesting and challenging molecules.

Experimental Details:

The fine sample of 5-Methyl-1H-tetrazole(5MTZ) was obtained from Lancaster Chemical Company.UK, with a stated purity of 99% and it was used as such without further purification.The FT-Raman Spectrum of PTZ was recorded using 1064 nm line of ND: YAG laser for excitation wavelength in the region 3500-100 cm^{-1} on Thermo Electron Corporation model Nexus spectrometer equipped with FT-Raman module accessory. The FT-IR

Spectrum of the title compound was recorded in the region 4000-400 cm^{-1} on Perking Elmer Spectrophotometer in KBr pellet.

Computational Details:

The combination of Vibration spectra with quantum chemical calculation is effective for understanding the fundamental mode of vibration of the compound. The structural characteristic, stability and energy of the compound under investigation are determined by DFT with the three-parameter hybrid functional (B_3) for the exchange part and the Becke Three Lee Yong-Pare (LYP) and 6-31G, 6-311+G basis sets with Gaussian 09 Program Package. The Cartesian representation of the theoretical force constants has been compound at the fully optimized geometry by assuming the molecule belongs to C_1 point group symmetry. The Transformation of force field from Cartesian to internal local symmetry coordinates, the scaling, and the subsequent normal coordinate analysis (NCA) Calculation of potential energy distributions (PED) has been done on a PC with the VEDA program.

Geometrical parameter.

The calculated C-N distances are $N1-C7 = 1.36 \text{ \AA}$, $N4-C5 = 1.34 \text{ \AA}$, this value indicate that the bond $N4-C5$ is stronger than the bond $N1-C7$ and these values indicate that the bond distances were found to be much smaller than the average value for a single C-N bond (1.47 \AA) [7]. The bond lengths of $N3-N4$, $N1-N2$ were found to be elongated to 1.40 \AA , 1.39 \AA respectively, compared to $N2-N3$ values of 1.32 \AA . Because bond order of $N2-N3$ is higher than $N3-N4$, $N1-N2$ bond order [8]. table-1

report the detailed data of geometrical optimization of the isolated title molecule. Functional group methyl substituted in ring structure with C5 atom which made longest bond length in that molecule structure because C-C bond shaped a nonpolar covalent bond[9] and the hyper conjugation causes the interaction of the orbital of the methyl group with the π orbital of a ring. in methyl group ,C-H bond length 1.10Å, (6-31G), 1.09 Å, (6-311+G) are good agreement with other literature values 1.09 Å [10] 1.08 Å, 1.09 Å [11] 1.09 Å [12]. this cooperation caused to discharging electronic charge from methyl group[13]. highest bond angle occurred at C5-N1-H6 whereas lowest bond angle occurred at N1-N2-N3.

Electronic properties

To explain several types of reactions and for predicting the most reactive position in conjugated systems, molecular orbital and their properties such as energy are used [14]. The highest occupied molecular orbital (HOMO) and lowest unoccupied molecular orbital (LUMO) are the most important orbital in a molecule. The eigen values of HOMO and LUMO and their energy gap reflect the biological activity of the molecule. A molecule having a small frontier orbital gap is more polarizable and is generally associated with a high chemical reactivity and low kinetic stability [15,16]. HOMO, which can be thought the outer orbital containing electrons, tends to give these electrons as an electron donor and hence the ionization potential is directly related to the energy of the HOMO. On the other hand LUMO can accept electrons and the LUMO energy is directly related to electron affinity [17]. Two important molecular orbital (MO)

were examined for the title compound, the highest occupied molecular orbital (HOMO) and the lowest unoccupied molecular orbital (LUMO) which are given in Fig. 3. In the title compound, the HOMO of π nature is delocalized over the tetrazole ring. By contrast, the LUMO is located over the tetrazole ring and methyl group. For understanding various aspects of pharmacological sciences including drug design and the possible ecotoxicological characteristics of the drug molecules, several new chemical reactivity descriptors have been proposed. Conceptual DFT based descriptors have helped in many ways to understand the structure of molecules and their reactivity by calculating the chemical potential, global hardness and electrophilicity. Using HOMO and LUMO orbital energies, the ionization energy and electron affinity can be expressed as: $I = E_{\text{HOMO}}$, $A = E_{\text{LUMO}}$. table shows global reactor values of the title compound. It is seen that the chemical potential of the title compound is negative and it means that the compound is stable. They do not decompose spontaneously into the elements they are made up of. The hardness signifies the resistance towards the deformation of electron cloud of chemical systems under small perturbation encountered during chemical process. The principle of hardness works in Chemistry and Physics but it is not physical observable. Soft systems are large and highly polarizable, while hard systems are relatively small and much less polarizable.

Molecular electrostatic potential (MEP)

MEP is related to the ED and is a very useful descriptor in understanding sites for electrophilic and nucleophilic reactions as

well as hydrogen bonding interactions [18,19]. The electrostatic potential $V(r)$ is also well suited for analyzing processes based on the “recognition” of one molecule by another, as in drug-receptor, and enzyme–substrate interactions, because it is through their potentials that the two species first “see” each other [20,21]. To predict reactive sites of electrophilic and nucleophilic attacks for the investigated molecule, MEP at the B3LYP level optimized geometry was calculated. The different values of the electrostatic potential at the MEP surface are represented by different colours: red, blue and green represent the regions of most negative, most positive and zero electrostatic potential respectively. The negative electrostatic potential corresponds to an attraction of the proton by the aggregate electron density in the molecule (shades of red), while the positive electrostatic potential corresponds to the repulsion of the proton by the atomic nuclei (shade of blue). The negative (red and yellow) regions of MEP were related to electrophilic reactivity and the positive (blue) regions to nucleophilic reactivity (Fig. 4). From the MEP it is evident that the negative charge covers the N atoms which presence in tetrazole group. the positive region is over the H atoms. The value of the electrostatic potential is largely responsible for the binding of a substrate to its receptor binding sites since the receptor and the corresponding ligands recognize each other at their molecular surface [22,23].

NLO properties

Nonlinear optics deals with the interaction of applied electromagnetic fields in various materials to generate new

electromagnetic fields, altered in wavenumber, phase, or other physical properties [24]. Organic molecules able to manipulate photonic signals efficiently are of importance in technologies such as optical communication, optical computing, and dynamic image processing [25,26]. In this context, the dynamic first hyperpolarizability of the title compound is also calculated in the present study. The first hyperpolarizability (b_0) of this novel molecular system is calculated using DFT method, based on the finite field approach. In the presence of an applied electric field, the energy of a system is a function of the electric field. First hyperpolarizability is a third rank tensor that can be described by a $3 \times 3 \times 3$ matrix. The 27 components of the 3D matrix can be reduced to 10 components due to the Kleinman symmetry [27]. The components of b are defined as the coefficients in the Taylor series expansion of the energy in the external electric field. When the electric field is weak and homogeneous, this expansion become

$$E = E_0 - \mu_\alpha F_\alpha - 1/2 \alpha_{\alpha\beta} F_\alpha F_\beta - 1/6 \beta_{\alpha\beta\gamma} F_\alpha F_\beta F_\gamma + \dots$$

Where E_0 is the vitality of the unperturbed atoms, F_α the field at the source μ_α , $\alpha_{\alpha\beta}$ and $\beta_{\alpha\beta\gamma}$ are the segments of dipole moment, polarizability and the first order hyper polarizabilities. The aggregate static dipole moment (μ), polarizability (α), anisotropy polarizability ($\Delta\alpha$) and the mean first order hyperpolarizability (β_{tot}) utilizing x, y, z , The segments are characterized as follows, The calculated first hyperpolarizability of the title compound is 0.3199×10^{-30} esu/6-31G, 0.3458×10^{-30} esu/6-311+G. The calculated hyperpolarizability of the title compound is superior than that of the standard NLO

material urea (0.13×10^{-30} esu) [28]. We conclude that the title compound is an attractive object for future studies of nonlinear optical properties.

Mulliken Atomic charge

The Mulliken atomic charge calculation has important role in the application of quantum mechanics calculations to molecular system: the atomic charge calculation of molecule plays an important role [28]. The electron distribution in 5MTZ is compared in two different quantum chemical methods and the sensitivity of the calculated charges to charge in the choice of methods is studied. By determining the electron population of each atom in the define basis function, the Mulliken charges are calculated. An estimated Mulliken charges at both levels are listed in Table 3. The results can be represented in graphical form as given in Fig 7. In this molecule all the hydrogen atoms have got positive charge. N1, N3 and N4 have negative charge. Tetrazole carbon atom has negative charge and methyl carbon atom has positive charge.

Vibrational Assignment

The detailed vibrational data of the c1 point group title molecule were tabulated in table. The higher value of theoretical vibrations have been reduced by scaled factor 0.9555 for >1500 cm^{-1} , 0.9826 for <1500 cm^{-1} in 6-31G basis set. as well as 0.9642 for >1500 cm^{-1} , 0.9860 for <1500 cm^{-1} in 6-311+G basis set.

The C-H linear vibration in methyl group occurs in the range $3000 - 2900$ cm^{-1} [29]. The methyl groups vibrational frequencies depend upon the connecting atom. For example, the stretching

frequency of C-OCH₃ is higher than that of C-CH₃ [30]. The C-H vibration frequencies also differ in their position. K. Parimala et al [31] assigned asymmetric C-H stretching frequency band at 2943 cm^{-1} , 2896 cm^{-1} and 2940 cm^{-1} , 2900 cm^{-1} respective in the FT-IR and FT-Raman. Other literature values assigned to the frequency band stretching for CH₃ molecule is 2833 cm^{-1} , 2875 cm^{-1} , 2991 cm^{-1} in FT-IR 2937 , 2975 cm^{-1} in FT-Raman [29], 2967 cm^{-1} , 2925 cm^{-1} in FT-IR, 2976 cm^{-1} , 2930 cm^{-1} in FT-Raman [32]. In this investigation all the vibration frequencies of the methyl group are in accordance with literature values those found in the characteristic group frequency as shown in Table V. The calculated values by B3LYP methods are fit with experimental values.

NH stretching is in the region $3500-3400$ cm^{-1} [33] and theoretically assigned at 3490 cm^{-1} and 3458 cm^{-1} [34]. In this molecule, in this work, the NH band occurred at 3420 cm^{-1} in FT-IR, 3550 cm^{-1} in FT-Raman. Theoretically, this band observed at 3535 cm^{-1} (6-31G), 3553 cm^{-1} (6-311+G).

B3LYP computation gives mode arising from the N-N stretching at 1162 cm^{-1} in 6-31G and 1162 cm^{-1} in 6-311+G basis set corresponding to the peak at 1113 cm^{-1} in IR spectrum. The C-N vibrations is a very critical task, since the mixing of vibrations is possible in this region. Silverstein et al. [35] attributed C-N stretching absorption in the region $1266-1382$ cm^{-1} for aromatic amines. In benzamide the band observed at 1368 cm^{-1} is assigned to the CN stretching band [36]. In 1,2,4-triazole the band observed at 1390 and 1327 cm^{-1} are assigned to CN stretching [37]. The C-N stretching modes

are reported in the range 1000–1400 cm⁻¹ [38] and in the present case these bands are assigned at 1008, 1354, 1508 (6-31G) 1007,1345, 1510 (6-311+G) cm⁻¹ theoretically. 1001, 1366, 1566 cm⁻¹ in IR and 1380, 1570 cm⁻¹ in Raman.

Natural Bond Analysis

The Natural bond orbital [39] analyzes is used to understand the delocalization of electron density and second order donor-acceptor energy. Typically, the stabilization of orbital interaction is high for higher energy differences between interacting orbitals. Effective donor and effective acceptor have this strong stabilization [40-43]. According to the second order perturbation approach, the stabilization energy is derived [44]. The energy from (donor) *i* → (acceptor) *j* is calculated as

$$E^2 = \Delta E_{ij} = q_i \frac{F(i, j)^2}{\varepsilon_j - \varepsilon_i}$$

Where, q_i is the donor orbital occupancy, ε_i , ε_j are diagonal elements (orbital energies) and $F(i, j)$ is the off-diagonal NBO Fock matrix element. The NBO analysis gives valuable information about the intra and inters molecule interaction of the molecule [45].

The current work summarizes second order perturbative calculation donor-acceptor interactions based on NBO. This analysis was carried out by observing all possible interaction between lewis and non-lewis NBOs and calculated their stabilization energy (E^2). Donor NBO (*i*), acceptor NBO (*j*) and stabilization energy (E^2) are

tabulated in Table 5.7. From this table, it is show that the interaction between the bonded N2-N3 (NBO 55) and N4-C5 antibond (NBO 58) gives the strongest stabilization, 27.74 kcal/mol and also, lonepair N1 (NBO 19) → N2-N3 antibond (NBO 55), lonepair N1 (NBO 19) → N4-C5 antibond (NBO 58), bonded N4-C5 (NBO 8) → N2-N3 antibond (NBO 55) has the highest stabilization energy are 18.98, 18.32, 16.27kcal/mol Respectively.

Conclusion

The present investigation thoroughly analyzed the HOMO-LUMO, and vibration spectra, both infrared and Raman of 5MTZ molecules with B3LYP method with standard 6-31G and 6-311+G basis sets. All the vibration bands are observed in the FT-IR and F-Raman spectra of the compound are assigned to various modes of vibration and most of the modes have wave numbers in the expected range. The complete vibration assignments of wave numbers are made on the basis of potential energy distribution (PED). The electrostatic potential surfaces (MEP) together with complete analysis of the vibration spectra, both IR and Raman and help to identify the structure and symmetry. The excellent agreement of the calculated and observed vibration spectra reveals the advantages over the other method. Finally, calculated HOMO-LUMO energies show that the charge transfer occurs in the molecule, which are responsible for the bioactive properly of the biomedical compound 5MTZ.

References

- [1]. Jack Peter Green, Carl L. Johnson, and Sungzong Kang. *Annu. Rev. Pharmacol.* 1974.14:319-342. Downloaded from www.annualreviews.org
- [2]. S. Wang, Z. Fang, Z. Fan, D. Wang, Y. Li, X. Ji, X. Hua, Y. Huang, T. Kalinina, V. Bakulev, Y. Morzherin, *Chinese Chem. Lett.*, 2013; 24: 889.
- [3]. H. Kavitha, N. Balasubramanian, *Ind. J. Chem. Tech.*, 2002; 9: 361.
- [4]. K. Chauhan, P. Singh, V. Kumar, P. Shukla, M. Siddiqi, P. Chauhan, *Eur. J. Med. Chem.*, 2014; 78: 442. 7. S. George, P. Shanmugapandiyam, *Int. J. Chem Tech Res.*, 2013; 5: 2603.
- [5]. S. Rostom, H. Ashour, H. Abd El Razik, A. Abd El Fattah, N. El-Din, *Bioorg. Med. Chem.*, 2009; 17: 2410.
- [6]. R. Herbst, C. Roberts, H. Givens, E. Harvill, *J. Org. Chem.*, 1952; 17: 262. 10. D. Wu, R. Herbst, *J. Org. Chem.*, 1952; 17: 1216.
- [7]. A.F. Holleman, E. Wiberg, N. Wiberg, in: W. de Gruyter (Ed.), *Lehrbuch der Anorganischen Chemie*, Berlin, New York, 2007.
- [8]. **A.Ramu**, M.K. Murali, M.karnan, M.Karunanithi. *Journal of Information and Computational Science*. ISSN: 1548-7741. Volume 9 Issue 11 – 2019.P: 1290- 1314. DOI: <http://www.joics.org/gallery/ics-1805.pdf>.
- [9]. D.Durgadevi,S.Manivarman,S.Subashchandrabose.j.Karbala *International Journal Of Modern Science* 3 (2017) 18-28
- [10]. V.Balachandran,A.Lakshmi,A.Jana ki.j.Mol Struct 1013(2012)75-85
- [11]. H.Tanaka, H.Takashima, M.Ubasawa, K.Sekiya, I.Nitta, M.Baba, S.Shigeta, R.T.Walker, E.De Clercq, T.Miyasaka, *J. Med. Chem.* 35 (1992)337-345
- [12]. V.Balachandran,A.Lakshmi,A.Jana ki.j.Spectrochimica Acta Part A 81(2011) 1-7
- [13]. A.Natraj,V.Balachandran,T.Karthick,j.Mol.Struct.1022(2012)94-108
- [14]. N. Choudhary, S. Bee, A. Gupta, P. Tandon, *Comp. Theor. Chem.* 1016 (2013) 8– 21.
- [15]. N. Sinha, O. Prasad, V. Narayan, S.R. Shukla, *J. Mol. Simul.* 37 (2011) 153– 163.
- [16]. D.F.V. Lewis, C. Loannides, D.V. Parke, *Xenobiotica* 24 (1994) 401–408.
- [17]. B. Kosar, C. Albayrak, *Spectrochim. Acta* 78 (2011) 160–167.
- [18]. E. Scrocco, J. Tomasi, *Adv. Quantum Chem.* 11 (1979) 115–121.
- [19]. F.J. Luque, J.M. Lopez, M. Orozco, *Theor. Chem. Acc.* 103 (2000) 343– 345.
- [20]. P. Politzer, J.S. Murray, in: D.L. Beveridge, R. Lavery (Eds.), *Theoretical Biochemistry and Molecular Biophysics: A Comprehensive Survey*, Protein, vol. 2, Adenine Press, Schenectady, New York, 1991.
- [21]. E. Scrocco, J. Tomasi, *Curr. Chem.* 42 (1973) 95–170.
- [22]. H. Kobinyi, G. Folkers, Y.C. Martin, *3D QSAR in Drug Design*, Recent Advances, vol. 3, Kluwer Academic Publishers., 1998.
- [23]. S. Moro, M. Bacilieri, C. Ferrari, G. Spalluto, *Curr. Drug Discovery Technol.* 2 (2005) 13–21.
- [24]. Y.R. Shen, *The Principles of Nonlinear Optics*, Wiley, New York, 1984.
- [25]. P.V. Kolinsky, *Opt. Eng.* 31 (1992) 11676–11684.
- [26]. D.F. Eaton, *Science* 25 (1991) 281–287.

- [27]. D.A. Kleinman, Phys. Rev. 126 (1962) 1977–1979.
- [28]. R.S. Mulliken, Electronic Population Analysis on LCAO-MOMolecular Wave Functions., J. Chem. Phys. 23 (1995) 1833-1840.
- [29]. A.Natraj,V.Balachandar,T.Karthick . J.mol struc 1022(2012)94-108.
- [30]. P.Vennila,M.Govindaraju,G.Venkatesh,C.Kamal J.mol structure.1111(2016)151-156.
- [31]. K.Parimala,V.Balachandran, Spectrochim.Acta 81A(2011) 711-723
- [32]. M.karnan,V.Balachandran,M.Murugan, Spectrochim.Acta A:mol and biomol Spec 96(2012) 51-62
- [33]. L.J.Bella my. *The IR Spectra of complex Molecules*, John Wiley and sons, New York, 1975.
- [34]. R.Minitha, Y.S.Mary, H.T.Varghese, C.Y.Panicker, R.Rauindran, K.Raju, V.M.Nair, FT-IR, FT -Raman and computational study of 1H-2, 2-dimethyl-3H-phenothazin- 4[IOH]- one, J.Mal, struct.985(2011)316-322.
- [35]. R.M. Silverstein, G.C. Bassler, T.C. Morrill, Spectrometric Identification of Organic Compounds, fifth ed., John Wiley and Sons Inc., Singapore, 1991.
- [36]. R. Shanmugam, D. Sathyanarayana, Spectrochim. Acta 40 (1984) 764–773.
- [37]. S. Genc, N. Dege, A. Cetin, A. Cansiz, M. Sekerci, M. Dincer, Acta Crystallogr. E60 (2004) 1340–1342.
- [38]. S. Kundoo, A.N. Banerjee, P. Saha, K.K. Chattopadhyay, Mater. Lett. 57 (2003) 2193–2197.
- [39]. S. Muthu, J. Uma Maheswari, Tom Sundius. Spectrochimica acta part A.Molecular And Biomolecular spectroscopy 106, (2013)299-309.
- [40]. A. E. Reed, F. Weinhold. J. Chem. Phys. 83 (1985) 1736-1740.
- [41]. A. E. Reed, R. B. Weinstock, F. Weinhold. J. Chem. Phys. 83 (1985) 735-746.
- [42]. A. E. Reed, F. Weinhold. J. Chem. Phys. 78 (1983) 4066-4073.
- [43]. J. P. Foster, F. Weinhold. J. Am. Chem. Soc. 102 (1980) 7211-7218.
- [44]. P. Singh, S. S. Islam, H. Ahmad, A. Prabakaran. J. Mol. Struct. 1154 (2018) 39-50.
- [45]. K. R. Santhy et al. J. Mol. Struct. (2018). DOI.10. 1016/j. molstruc. 2018. 09. 058.

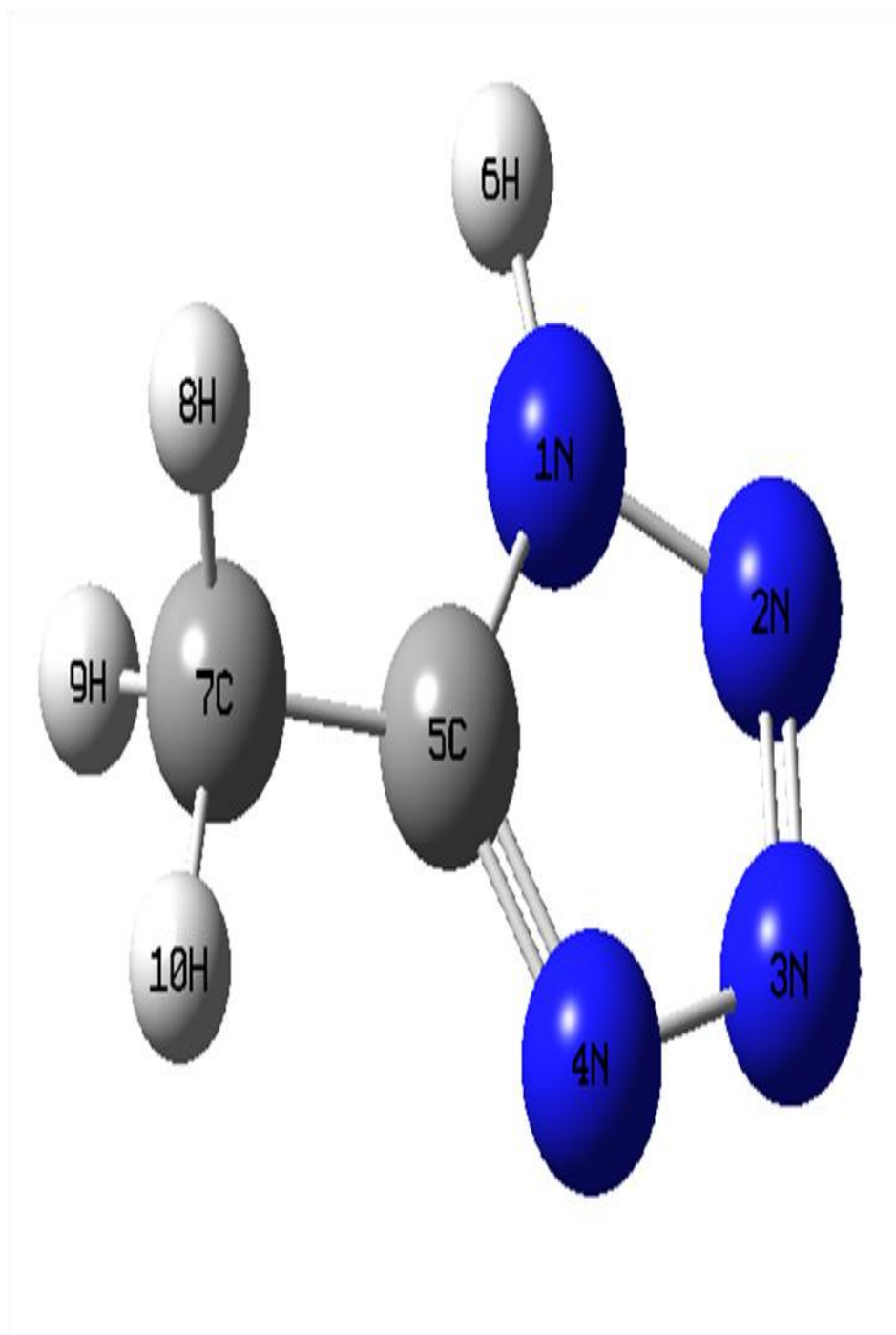


Fig 1. The theoretical geometry structure and atomic numbering scheme of 5-Methyl-1H-tetrazole (5MTZ).

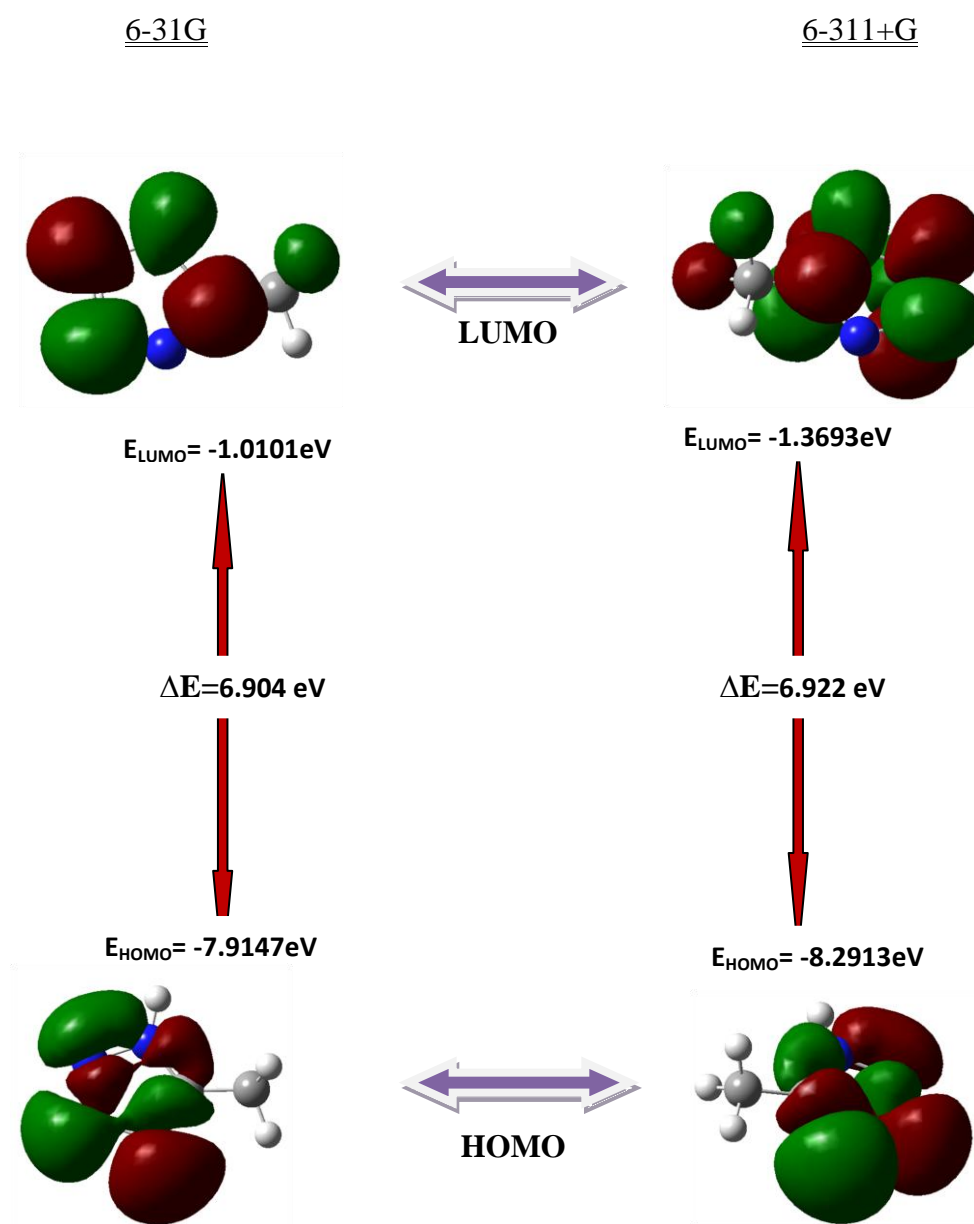


Fig 2: The atomic orbital compositions of the frontier molecular orbital for 5-Methyl-1H-tetrazole (5MTZ).

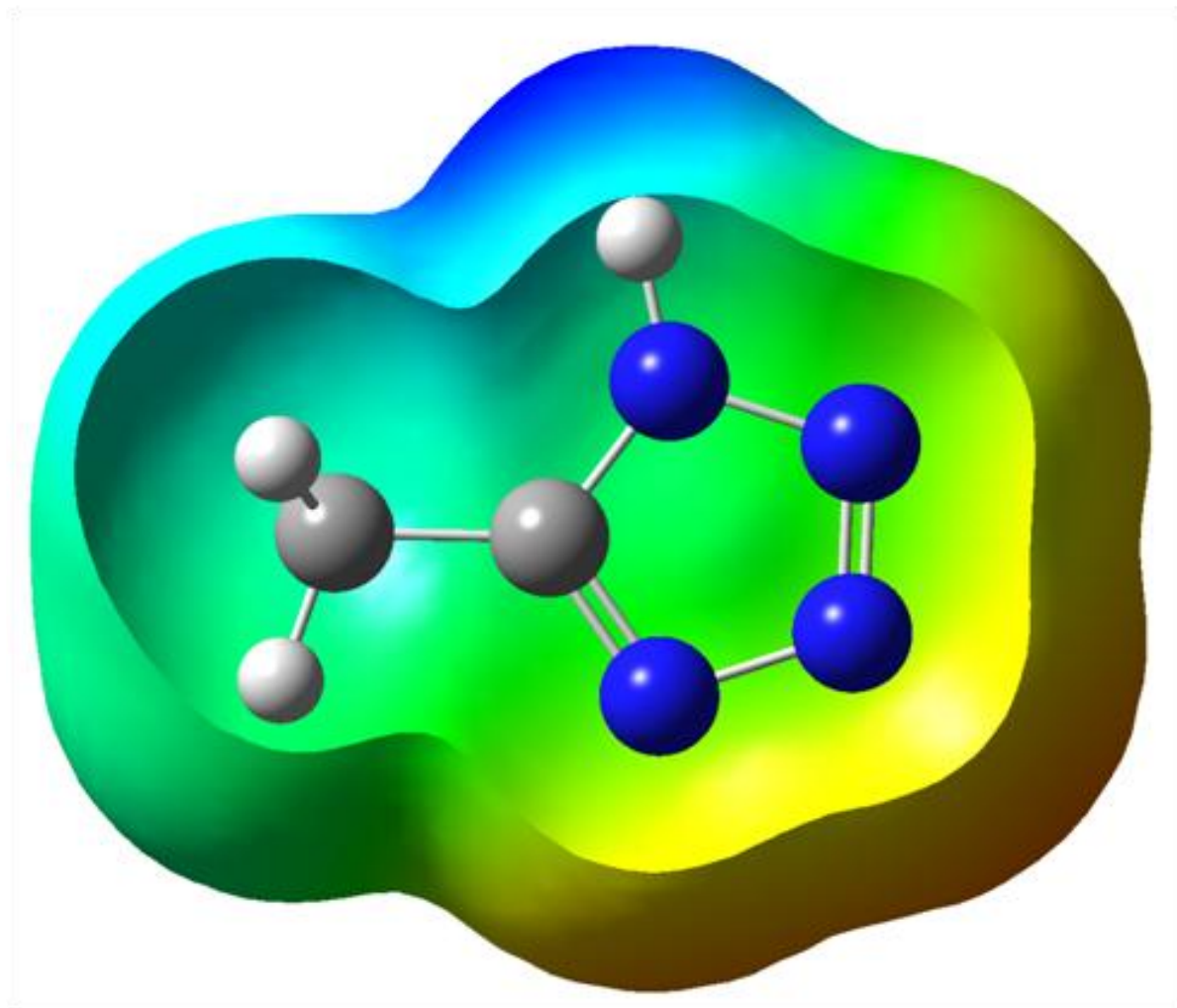


Fig 3. The total electron density surface mapped with of 5-Methyl-1H-tetrazole (5MTZ).

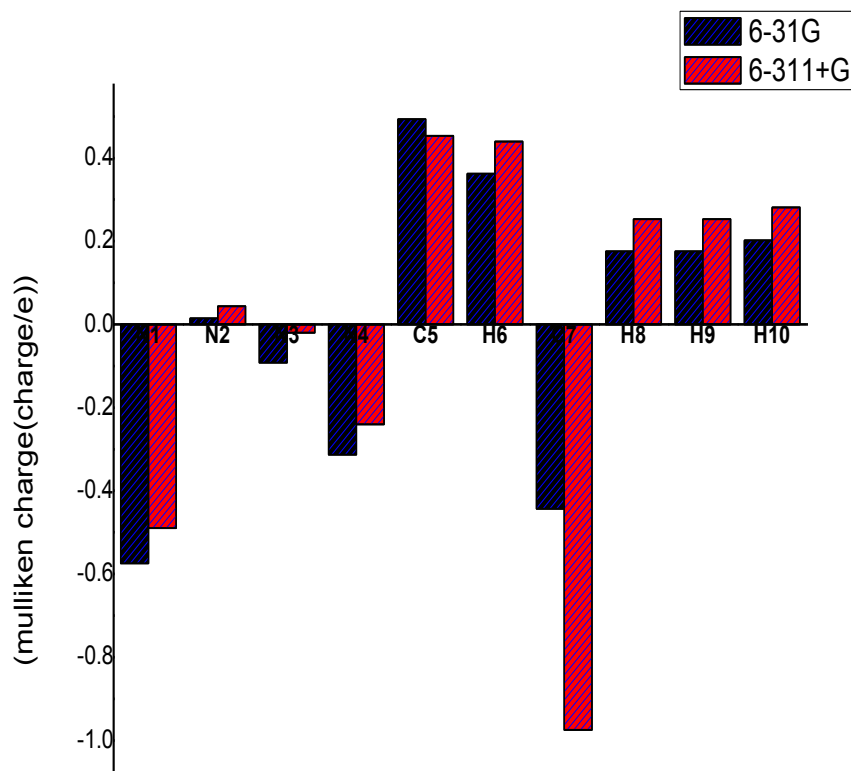


Fig 4 Bar diagram representing the Mulliken atomic charge distribution of 5-Methyl-1H-tetrazole (SMTZ).

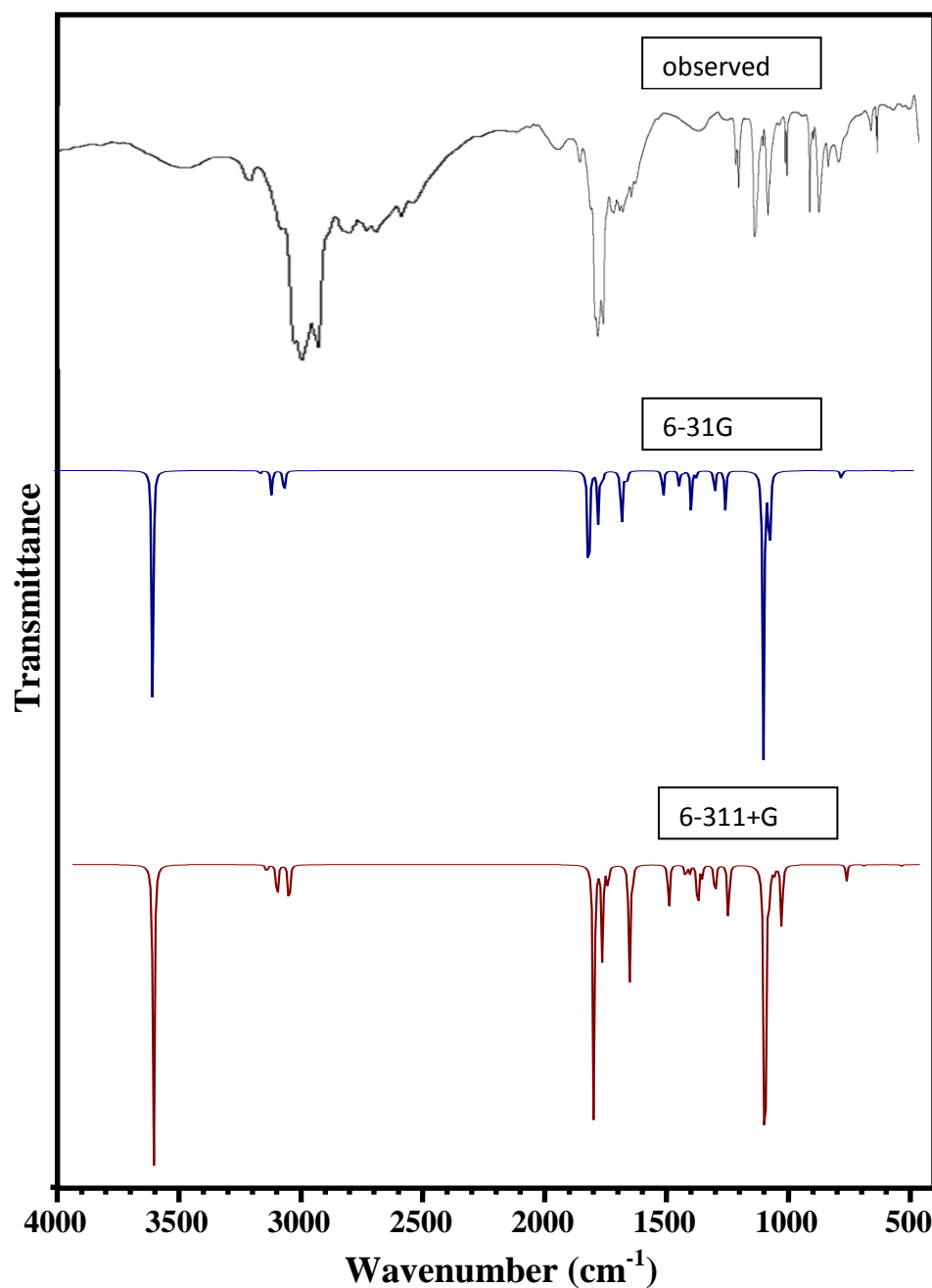


Fig 5. Comparative representation of FT-IR spectra for **5-Methyl-1H-tetrazole (5MTZ)**.

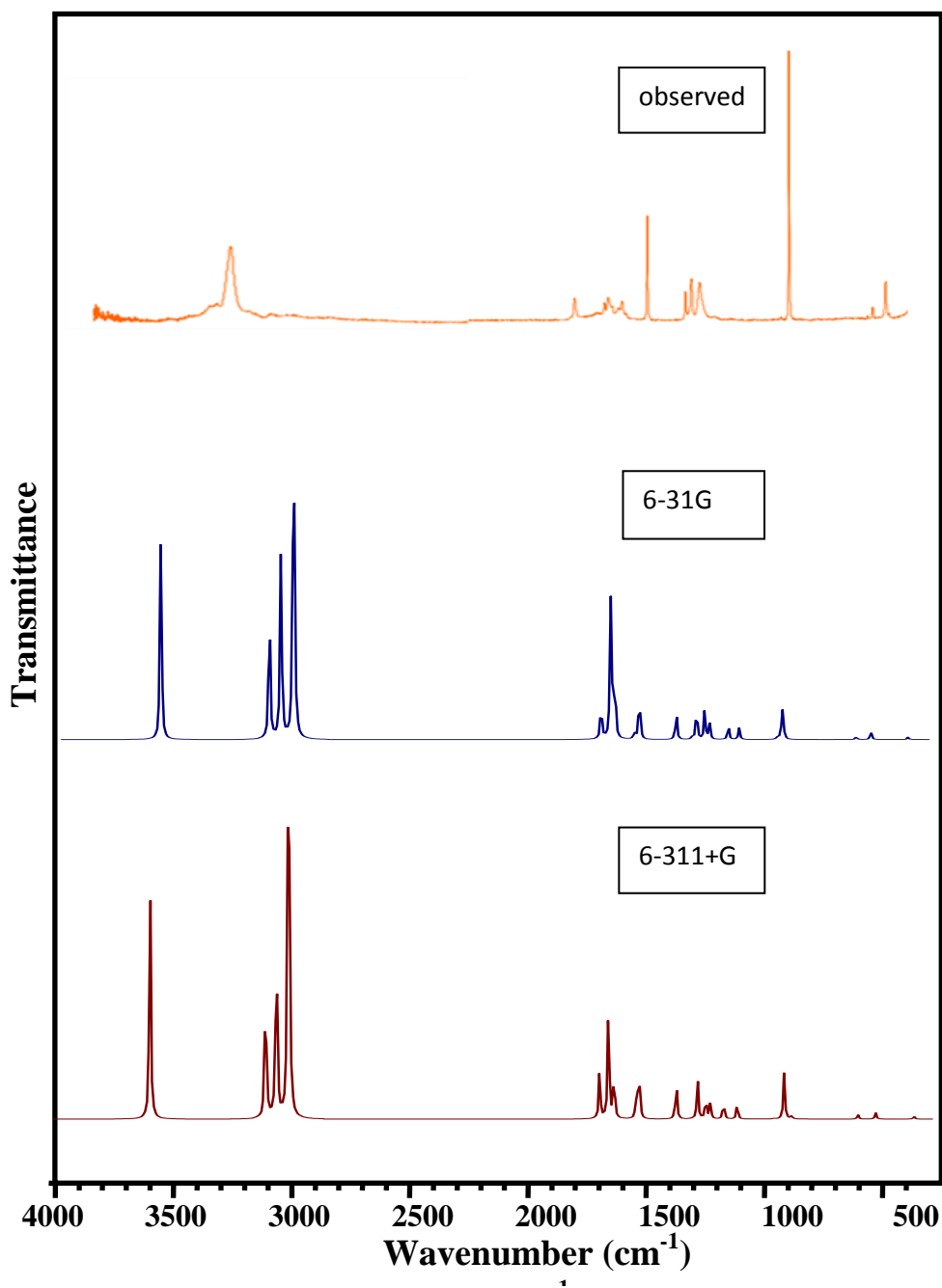


Fig 6. Comparative representation of FT-Raman spectra for **5-Methyl-1H-tetrazole (5MTZ)**.

Table 1: Geometry Optimization Parameter of 5-Methyl-1H-tetrazole (5MTZ) based on B3LYP/6-31G and B3LYP/6-311+G method and basis set.

Atom	BondLength(Å)		Atom	BondAngle(°)	
	6-31G	6-311+G		6-31G	6-311+G
C5-C7	1.49	1.48	C5-N1-H6	130.75	130.85
N3-N4	1.40	1.40	N1-C5-C7	126.12	126.10
N1-N2	1.39	1.39	N4-C5-C7	125.90	126.01
N1-C5	1.36	1.36	N2-N1-H6	119.91	119.60
N4-C5	1.34	1.34	C5-C7-H8	111.56	111.62
N2-N3	1.32	1.32	C5-C7-H9	111.54	111.57
C7-H9	1.10	1.09	N2-N3-N4	110.77	110.54
C7-H8	1.10	1.09	N2-N1-C5	109.35	109.55
C7-H10	1.09	1.09	C5-C7-H10	108.65	108.81
N1-H6	1.01	1.00	H8-C7-H10	108.47	108.30
			H9-C7-H10	108.47	108.29
			H8-C7-H9	108.06	108.15
			N1-C5-N4	107.98	107.89
			N3-N4-C5	106.36	106.49
			N1-N2-N3	105.54	105.54

Table 2: HOMO-LUMO energy (eV) and other related properties of 5-Methyl-1H-tetrazole (5MTZ) based on B3LYP/6-31G and B3LYP/6-311+G method and basis set.

Parameters	6-31G (eV)	6-311+G (eV)
Homo(I)	-7.9147	-8.2913
Lumo(A)	-1.0101	-1.3693
Energy gap(ΔE)	6.9046	6.9220
Electronegativity	4.4624	4.8303
Global hardness	3.4523	3.4610
Global softness(eV^{-1})	0.2897	0.2889
Chemical potential	-4.4624	-4.8303
Electrophilicity	2.8840	3.3706

Table 3: Dipole moment(μ), Polarizability(α), Anisotropy polarizability($\Delta\alpha$) and First order polarizability(β_{tot}) of 5-Methyl-1H-tetrazole (5MTZ) based on B3LYP/6-31G and B3LYP/6-311+G method and basis set.

Parameters	6-31G	6-311+G
μ_x	-4.7921	4.9639
μ_y	4.0155	4.1044
μ_z	0.0001	0.0003
α_{XX}	-37.5178	-38.5207
α_{YY}	-34.8592	-35.9312
α_{ZZ}	-34.6744	-35.4883
α_{XY}	0.054	0.0135
α_{XZ}	-0.001	-0.001
α_{YZ}	0.0002	0.0007
β_{XXX}	-23.2569	24.9565
β_{YYY}	21.6646	22.7176
β_{ZZZ}	0.0017	0.0013
β_{XYY}	-5.3476	5.8671
β_{XXY}	-0.165	-0.2122
β_{XXZ}	0.0009	-0.0028
β_{XZZ}	-0.6815	1.2008
β_{YZZ}	1.1585	1.5009
β_{YYZ}	-0.0006	0.0004
β_{XYZ}	-0.0007	-0.001
μ (debye)	6.2521	6.4410
α (esu)	-5.2812×10^{-24}	-5.4237×10^{-24}
$\Delta\alpha$ (esu)	65.0411×10^{-24}	66.7801×10^{-24}
β_{tot} (esu)	0.3199×10^{-30}	0.3458×10^{-30}

Table 4: Mulliken charge (charge/e) of 5-Methyl-1H-tetrazole (5MTZ) based on B3LYP/6-31G and B3LYP/6-311+G method and basis set.

Atom	6-31G	6-311+G
	Charge/e	
N1	-0.5748	-0.4897
N2	0.0143	0.0438
N3	-0.0924	-0.0203
N4	-0.3128	-0.2401
C5	0.4934	0.4534
H6	0.3618	0.4396
C7	-0.4437	-0.9744
H8	0.1759	0.2534
H9	0.1759	0.2534
H10	0.2023	0.2809

Table 5: Observed Frequency (cm⁻¹)- Theoretical Frequency (cm⁻¹) and Vibrational assignment with PED(%) of 5-Methyl-1H-tetrazole (5MTZ) based on B3LYP/6-31G and B3LYP/6-311+G method and basis set.

Specs	Observed Frequency(cm ⁻¹)		Theoretical Frequency(cm ⁻¹)				Vibrational assignment (PED %)
	FT-IR	FT-Raman	6-31G		6-311+G		
			Calc	scaled	Calc	Scaled	
A	3420	3550	3700	3535	3684	3553	v NH (100)
A	3146	-	3176	3035	3140	3028	v CH(86)+v CH(14)
A	2955	-	3121	2982	3090	2979	v CH(99)
A	2923	-	3060	2923	3032	2924	v CH(14)+v CH(86)
A	1566	1570	1578	1508	1566	1510	v NC(23)+v CC(23)
A	1464	-	1532	1464	1526	1471	β HCH(78)+τ HCCN(21)
A	-	-	1529	1461	1523	1469	β HCH(71)+τ HCCN(21)
A	1409	1410	1469	1444	1465	1444	β HCH(97)
A	1366	1380	1378	1354	1364	1345	v NC(30)+v NC(19)+β NNC(11)
A	1269	1270	1355	1331	1350	1331	v CC(14)+β HNN(57)
A	1113	1105	1182	1162	1178	1162	v NN(73)
A	1089	1090	1106	1087	1099	1084	β HCH(20)+τ HCCN(60)+τ HCCN(10)
A	1064	1070	1087	1068	1080	1065	v NC(32)+v NC(14)+β NCN(14)
A	-	-	1049	1031	1042	1027	β NNN(71)
A	1001	-	1026	1008	1022	1007	v NC(11)+β HCH(15)+β NNC(15)
A	928	-	939	922	961	947	v NN(68)+β NCN(11)
A	723	-	888	872	897	885	v NC(19)+β NCN(43)+β NNN(16)
A	690	-	711	699	726	716	τ NNNC(31)+τ NNCN(58)
A	683	-	706	694	703	694	τ HNNN(79)+τ NNNC(19)
A	-	-	686	674	681	672	v NC(10)+v CC(52)+β NCN(11)
A	-	490	679	667	646	637	τ HNNN(15)+τ NNNC(44)+τ NNCN(19)

A	-	330	339	333	341	336	β CCN(86)
A	-	270	270	265	260	256	τ NNCN(19)+ δ CNNC(65)
A	-	-	96	94	83	81	τ HCCN(77)+ δ CNNC(11)

Table 6: Natural Bond Orbital Calculation of 5-Methyl-1H-tetrazole (5MTZ)

S.No	Donor NBO (i)			Acceptor NBO (j)			E(2) kcal/mol	E(j)-E(i) a.u.	F(i,j) a.u.
1	55	BD	N2-N3	58	BD*	N4-C5	27.74	0.04	0.04
2	19	LP	N1	55	BD*	N2-N3	18.98	0.34	0.34
3	19	LP	N1	58	BD*	N4-C5	18.32	0.38	0.38
4	8	BD	N4-C5	55	BD*	N2-N3	16.27	0.3	0.3
5	21	LP	N3	51	BD*	N1-N2	12.15	0.68	0.68